Physical Sciences

Pak J Sci Ind Res 2000 43 (2) 73-82

Petrography and Geochemistry of Kora Gypsum Deposit, Daudkhel, District Mianwali

Shahid Naseem[a], Shamim Ahmed Sheikh[a], M Qutbuddin[b] and Mussarat Akhtar*

[a]*Department of Geology, University of Karachi, Karachi, Pakistan*

[b]*PCSIR Laboratories Complex, Off University Road Karachi, Pakistan*

(Received 6 November 1998, accepted 28 June 1999)

The Kora Gypsum Deposit (KGD) is present in the western Salt Range near Daudkhel in District Mianwali. Petrographic and geochemical studies of KGD have been made to evaluate the nature of deposit and characteristics of the depositional environment. The gypsum grades into Sakesar limestone of Upper Eocene age. It is inferred that KGD is a sulphate facies of Sakesar limestone, formed in a barred basin. Trace element analyses of gypsum and limestone show nearly similar distribution patterns, indicating same geochemical environment. The low Mg, poor Fe and absence of K from the gypsum samples indicate Deep Basin Deep Water (DBDW) condition. The presence of clay, high chalcophile elements (Zn, Cu and Ni) and sedimentary structures observable in the field also suggest a DBDW model. The thin section studies and geochemical investigations communicate that initially gypsum was precipitated either due to evaporation or mixing of different brines. Dehydration of gypsum into anhydrite occurred during Miocene due to thick accumulation of overlying Siwaliks. The Pliocene Himalayan orogeny caused uplifting of the area and subsequent erosion and removal of overburden brought these anhydrite beds to near-surface conditions, where they were converted into gypsum due to rehydration from groundwater.

Key words: Gypsum, Petrography, Geochemistry, Depositional basin, Kora, Daudkhel.

Introduction

In Salt and Surghar Ranges gypsum and anhydrite deposits are associated with the rocks of Eocambrian-Cambrian and Lower Eocene age. Lower Eocene formations show distinctive facies change due to complex tectonics of the area. During Lower Eocene the Kohat-Potwar and Sulaiman provinces of the Indus Basin were separated by a barrier and as a result close depositional basins were developed (Latif and Iqbal 1980). Many evaporitic beds are present within Eocene succession. Sakesar limestone of Lower Eocene is well developed in the western Salt Range and in the Surghar Range. In Daudkhel area this limestone grades at places into gypsum.

Present study deals with the petrographic and geochemical studies of Kora Gypsum Deposit. Major and trace element geochemistry is carried out to discuss the nature and origin of the gypsum deposit. It is also aimed to elaborate its facies relationship with the Sakesar Limestone.

Materials and Methods

The area under study is situated in the western Salt Range near Daudkhel Industrial Complex, District Mianwali, Punjab (Fig 1). This location is close to Mari Indus and Daudkhel railway stations on the Kundian-Attock section of the Pakistan railway. A road from Mianwali to Kalabagh also passes close to these towns. Three isolated hills of gypsum deposits are located about 3 km northeast of Daudkhel railway station on both sides of Jaba Nala. Kora Gypsum Hill is situated north of Jaba Nala (Fig 2).

The sampling was carried out from the Kora Gypsum Hill, north of Jaba Nala (Fig 2). Fifteen successive samples were collected from bottom to top from the western wall of the main quarry of the Kora Gypsum Deposit (Fig 3). The gypsum bed were inclined at an angle of 90° towards east with variable thicknesses and physical characters. Sampling was made from those horizons that represent different hardness, colour and texture. Two samples of Sakesar limestone of Early Eocene (No. 16 and 17) were also collected from the adjoining bed to relate correspondence in trace elements geochemistry and facies analysis.

Amount of insoluble residue (IR), combined oxides of Fe and Al (R_2O_3), sulphate (SO_3), loss on ignition (LOI) and water of crystallization (H_2O) were determined gravimetrically. Calcium and magnesium were estimated by EDTA titration. Trace elements were estimated using an atomic absorption spectrophotometer (Hitachi Z-8000).

Thin sections of gypsum were studied with the help of Leitz microscope (Laborlux POL S). Photomicrographs of the selected

*Author for correspondence

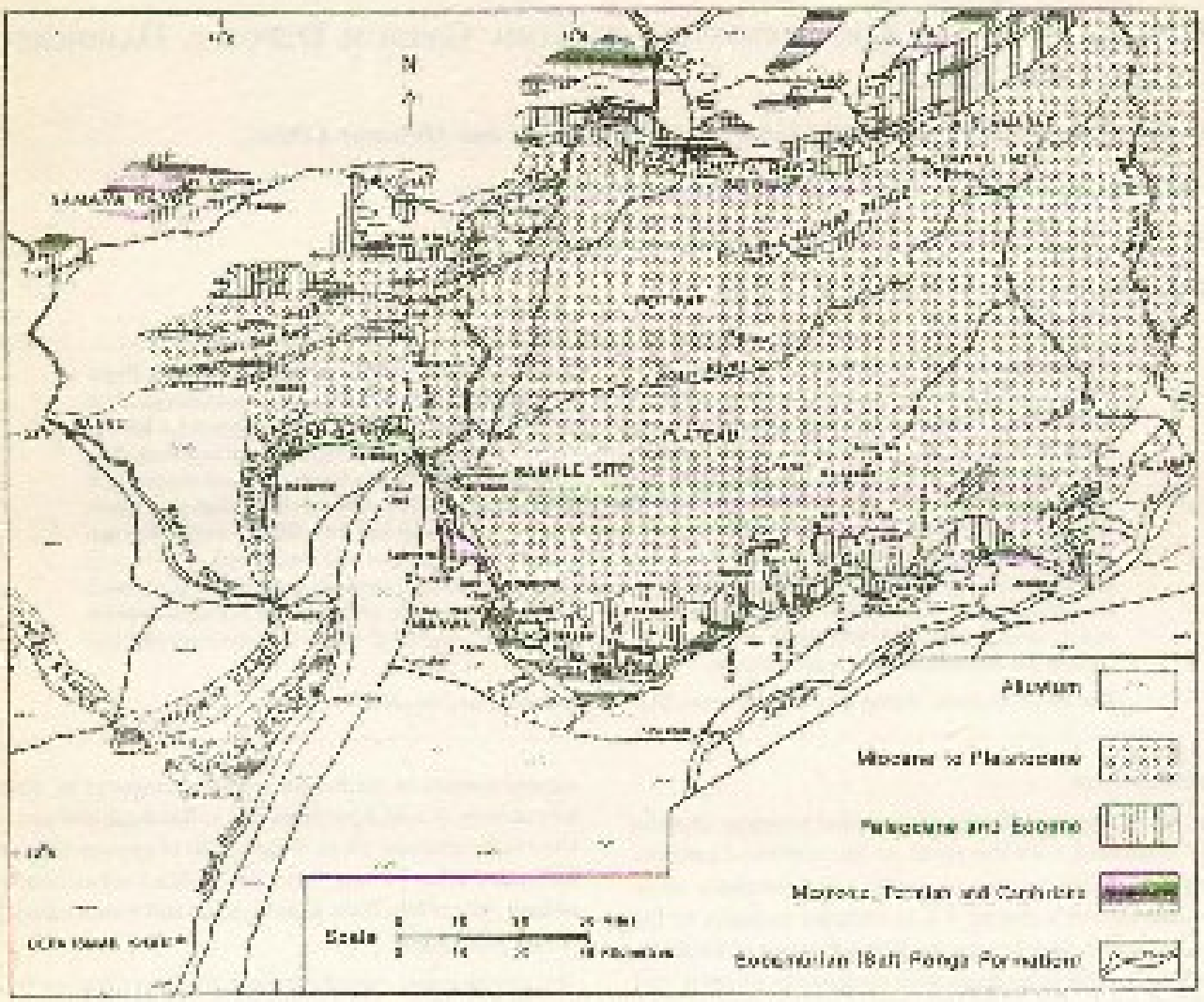

Fig 1 Location map of the Salt Range and adjoining areas. (Modified after Gee 1945).

samples was done with the help of Photocatalomat Wild Leitz (MPSV).

General geology. The oldest rocks exposed in the Salt Range are evaporites of late Precambrian to early Cambrian age. These are overlain by well exposed sequence of Cambrian, Permian, Triassic, Jurassic, Cretaceous, Paleocene and Neogene strata (Yeats et al 1984). In the study area, Precambrian to recent rocks are exposed with a number of unconformable and fault contacts (Fig 2). In Salt and Surghar Ranges lower Indus tectonics separated Kohat Potwar and Sulaiman provinces by means of a barrier. In this close basin salt, gypsum, anhydrite, shale and limestone were deposited. A total of nine formations of early Eocene are exposed in the vicinity of the area. There distribution is as follows: Ghazij formation in Dera Ismail Khan; Panoba shale, Shekhan formation, Bahadur Khel Salt and Jatta gypsum in Kohat; Nammal formation and Sakesar limestone in Salt and Surghar Ranges; Margala Hill limestone and Chorgali Formation in Nizampur Hill, Northern Potwar and Kalachitta areas. Sakesar limestone of early Eocene is well developed in the western Salt Range and the Surghar Range but in the Dandibel area, gypsum and anhydrite facies is developed at places instead of limestone.

Sakesar limestone consists dominantly of limestone with subordinate marl. It is cream to light grey coloured, nodular and fossiliferous. Considerable development of chert lenses in the upper part is also evident, specially in the Surghar Range. The marl is cream or light grey coloured and forms a persistent horizon near the top. Near Dandibel, Sakesar limestone is represented by gypsum and anhydrite which in fact is the sulphate facies within this formation. In the western Salt Range its thickness is 70m, in western Salt Range it is about 150m

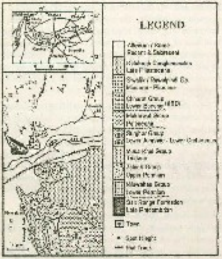

Fig 2 Geological map of the study area (Modified after Gee 1980).

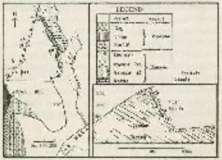

Fig 3 Detailed geological map and cross section of KGD showing sample locations (Modified after Alam and Khan 1982).

thick and in the Surghar Range its thickness varies between 200-300m. The *Sakesar* limestone is assigned an Early Eocene age based on foraminifera assemblage throughout the Salt Range (Latif and Iqbal 1985).The lower contact with the Nammal formation and upper contact with the Chorgali formation are conformable, while in the *Surghar* Range the formation is unconformably underlying by Siwalik group of Miocene to Pliocene age.

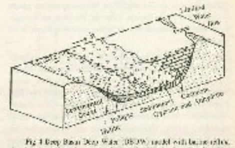

Fig 4 Deep Basin Deep Water (DBDW) model with basinal tallus showing deposition of gypsum in basin (Modified after Kendall 1992).

Structure. Structurally, the Salt Range is the result of tectonic forces imposed during the later phase of the Himalayan orogeny in Late Cenozoic (Gee 1989). The work of Burbank and Beck (1989) indicates that major upliftling in the Salt Range area took place during Early Pliocene. This uplifting event resulted from large scale thrusting related to the salt lubricated Potwar detachment.

The major fault of the area running across the strike of Salt Range is Kalabagh fault which is an active dextral wrench fault with a 16-19 km of strike-slip movement. This fault has been dated as 2.1-1.0 Ma (McDougall and Khan 1990). Near Isha Nala the Kalabagh fault splays out and forms two subparallel faults, Airwan and Dinghot faults (Fig 2). These faults form a lateral ramp extending to the base of Salt Range Potwar Plateau allochthon. Another important structural feature in the area is the Salt Range Thrust. It runs along the southern margin of the Salt Range, between Jhelum and Indus rivers. The thrust zone is largely covered by conglomerates but it is exposed in Kalabagh area (Kazmi and Jan 1997). The thrust has pushed the older rocks upon the tertiary sequence. As a result vertical tectonic slivers of the Salt Range, Permian and other tertiary formations occur at the north of Isha Nala.

Geological history. The Late Cretaceous regression of the Tethys Sea uplift and erosion gave rise to a major unconformity at Cretaceous-Tertiary (KT) boundary. During Paleocene, marine transgression resulted in the deposition of Hangu and Lockhart formations. In the late Paleocene, a lacustrine environment developed in the eastern and central Salt Range, resulting in the formation of coal deposits within Patala formation.

The Nammal, Sakesar and Chorgali formations of Early Eocene once witnessed marine condition. During Eocene to Oligocene, the area once again suffered epirogenic movements causing uplifting and erosion due to collision of

Indian Plate with the Eurasian Plate. No marine sedimentation occurred after Early Eocene. Miocene, Pliocene and Quaternary rocks were deposited in lacustrine and fluviatile environments (Gee 1989).

In the lower Eocene, the upper Indus Basin was tectonically active due to collision between Indian and Eurasian Plates. Uplifting caused separation of Kohistan province in the south-west and Kohat-Potwar province in the north-east. The Kohat-Potwar province became a close basin with a limited circulation (semi-open environment) (Ahmad and Kashmir Jamil and Iqbal 1960). This barrier basin was suitable for the accumulation of evaporite facies consisting of carbonate, gypsum, anhydrite and salt. Einsele (1992) has discussed and illustrated evaporitic facies model (Fig 4) that is generally developed in a humid basin. In this type of depositional setting, halite is restricted to the distal side of the basin. The seaward side is the suitable place for the calcareous facies. The central part of the basin is appropriate site for the accumulation of gypsum and anhydrite, represented by Bandichel gypsum deposits (DGD). In the study area Sakesar limestone (this model. The DGD is the sulphate facies of the Sakesar limestone, deposited in the deepest and central part of the basin.

Initially gypsum crystallizes in the form of polygonal rosettes in a deep humid basin due to supersaturation/evaporation. The deposition of Siwaliks in Miocene Pliocene caused enough overburden for dehydration of gypsum. Adams (1971) estimated 500 m overburden sufficient to dehydrate the gypsum into anhydrite. Jowett *et al* (1993) calculated ~400m depth for gypsum dehydration based upon pore fluid pressure, heat flow and thermal conductivity of the overlying Siwalik group. The anhydrite of the study area exposed due to Pliocene Pleistocene deformation. The addition of water molecules (water of crystallization) from groundwater to anhydrite is responsible for the formation of gypsum near the surface while at deeper parts anhydrite is still present, as also indicated by Ahmad and Khan (1962).

Reserves. Gypsum and anhydrite reserves in the Bandichel area have been estimated 45 million tons upto a depth of 30 m (Ahmad and Siddiqui 1959). However total reserves in the Salt Range area are about 138 million tons (Adam and Khan 1962).

Results and Discussion

Petrography. Out of 15 samples, 10 samples were selected for petrographic studies. This selection was made on the basis of difference in colour, grain size, degree of crystallization, intensity of replacement and presence of clay and iron oxides (Table 1). Photomicrographs (Fig 5) are included for precise and real presentation of petrographic properties of gypsum and anhydrite. The samples are mostly composed of anhydrite as granular aggregates or crystalline in nature and show replacements by gypsum. Crystallization increases towards top as from very fine to coarse crystals. Replacement of anhydrite with gypsum is obvious and is little in amount near the bottom and very high towards the top of the Kuna outcrop.

Clay is also present as thin laminae and filling in the cracks. The amount of clay increases from top to bottom of the section. Thin clay laminae between thick evaporite layers are marked for deep basin deposits (Goldsmith 1963). The absence of mudcracks and poor clay content also indicate deposition at deeper level. Specks and stains of iron are also present in a few samples. A few intersections of gypsum are also present. Table 1 presents degree of crystallization, replacement, presence of clay and iron minerals.

In thin section, sample 1 appears as irregular aggregate of anhydrite replaced with gypsum which is fine to medium grained (Fig 5A). Sample 2 consists of laminated layers of anhydrite, granular aggregate and fine grained layers of dirty brown clay are present in anhydrite (Fig 5B). Sample 3 shows thick brown layer within medium grained anhydrite. Few veins of anhydrite running across the laminations of clay and anhydrite are also visible (Fig 5C). Sample 6 seems to be coarse crystalline, more vein filling and layering is less noticeable. Sometimes veins are also visible (Fig 5D). Photomicrographs (Fig 5E & F) of samples 7 and 8 exhibit nearly similar pattern. Prominent lamination and replacement with gypsum is a common feature. Fine crystal aggregates of gypsum which have replaced anhydrite are common in samples 10 and 11. Brown clay is present without any pattern (Fig 5G & H). Samples 13 and 14 display relatively coarse crystals of gypsum. In this, replacement of anhydrite by gypsum is very distinct (Fig 5I).

Geochemistry. Composition and plots of major constituents of gypsum such as CaO, MgO, I.R., SiO_2 and R_2O_3 are given in Fig 6 and Table 2. The plot of CaO vs SO$_3$ shows clustering except in sample 3, which contains high amount of clay. This shows a good agreement between the two ions for gypsum formation. MgO shows variable enrichments (0.72-3.83%) against SO$_3$ values, which are nearly close (Fig 6). The plot of CaO vs MgO shows a vertical linear relationship. Mg rich brines may percolate in aragonite calcite sediments and cause dolomitization (Hsue 1990). The removal of Ca ions may cause high Mg/Ca ratio for the deep basin evaporites (Schmalz 1969). It is important to note that the plot of Ca/Mg vs Ca shows a gradual deepening of the basin during deposition of the Kuna Gypsum (Fig 6). The low Mg content in

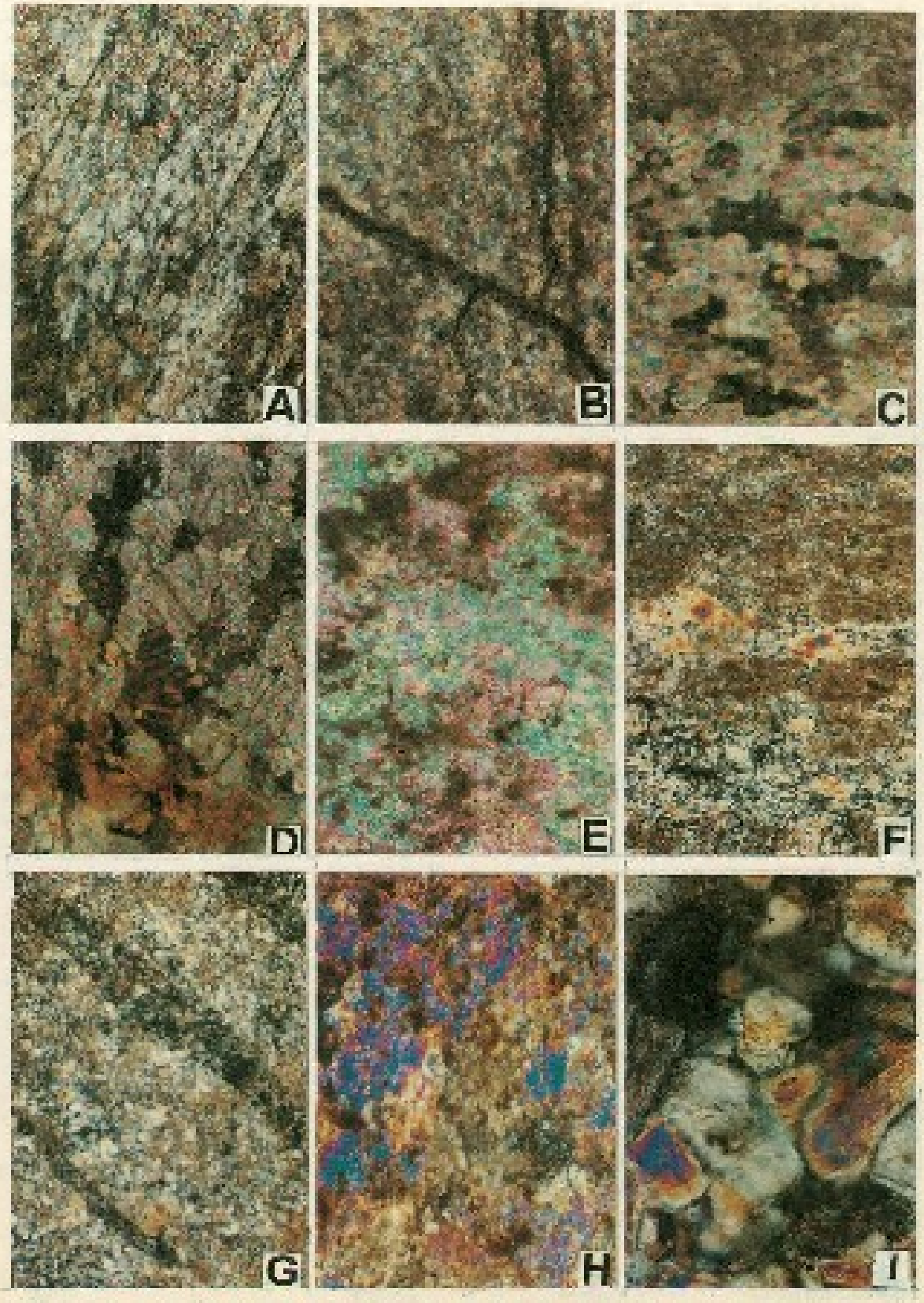

Fig 5. Photomicrographs of Kerang gypsum deposit. Cross nicols, x 50, except F is x 125

the study area also provides a good evidence for deep basin (Butler 1969). Dolomite is preferably seen form in shallow water. At higher depth CO_2 is more dissolved in water and unable the precipitation of dolomite because $MgCO_3$ is more soluble than $CaCO_3$ (Adams 1971).

The plots of IR vs CaO and MgO show different patterns. CaO shows clustering of population indicating nearly low influx of clay material except in sample 7. MgO does not show any relevance with clay. Probably this situation reflects no genetic relationship between them (Fig 6). Thin layers within evaporites are good sign for deep basin deposits. The distribution of R_2O_3 vs CaO and MgO is also quite similar to the above pattern (Fig 6).

Major and trace elements: The plots of major oxides and important trace elements (Fig 7) show a good agreement to depict depositional environment and change thereafter. CaO vs Sr, Fe, Al and Mn shows nearly similar vertical relationships (Fig 7). Trace elements show variable concentration at nearly close concentration of CaO indicating no genetic affinity at the time of gypsum deposition. Possibly these variations are due to post depositional changes, specially during successive dewatering and weathering. According to Goldschmidt (1958) variable enrichment of trace elements is characteristic of deep basin deposition. In the evaporite sequence, K minerals tend to crystallize at the last stage and hence K is poor in the gypsum. Not a single sample of the study area shows enrichment of K. Perhaps it is removed during dewatering from gypsum after burial. Metasomatic reactions may concentrate K after burial (Goldschmidt 1958). The present situation infers presence of no metasomatic activity in the area.

The concentration of trace elements is tabulated in Table 3. The concentration of Sr, the most important trace element

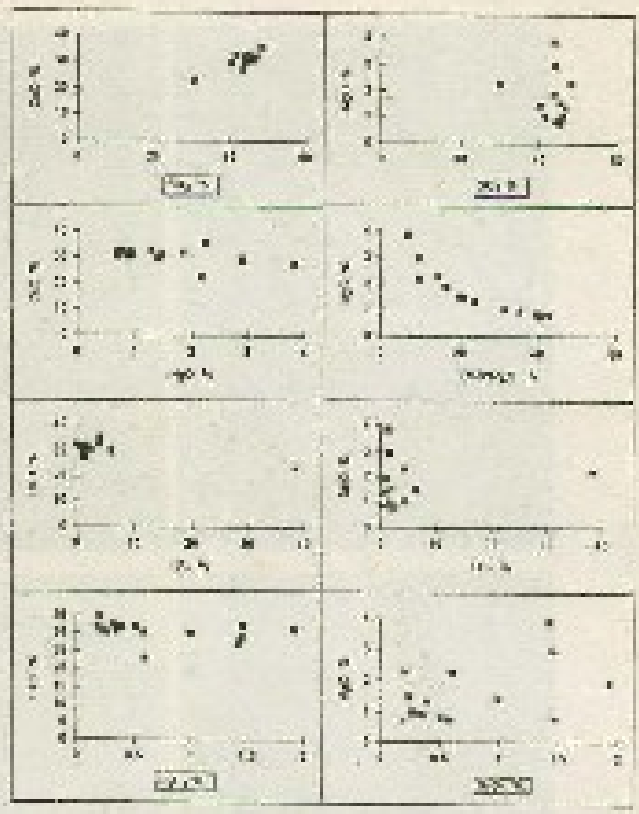

Fig 6. Degree of correspondence among major components.

in both limestone and gypsum, ranges between 338-2150 ppm. The average abundance of Sr in sea water is 8 ppm. The high concentration of Sr in the samples is probably due to high partition coefficient (PC) of Sr in contrast to other trace elements. The PC shows drastic increase with brine of high salinity. High growth rate of gypsum also increases PC of Sr (Kushner 1976). The other reason for high Sr enrich-

Table 1

Summary of the petrographic studies of Kurri Gypsum deposit

Sample No.	Grain size (mm)	Crystalline/ granular	Replacement by gypsum	Clay minerals	Iron minerals
1	0.125-0.5	Granular	Partial	5	<1
2	0.125-0.25	Granular	No	25	5
3	0.25-0.75	Crystalline	No	5	5
5	1.0-1.25	Crystalline	Partial	20	<1
7	0.125-0.25	Granular	No	40	<1
8	0.125-0.25	Crystalline	Considerable	40	<1
10	0.125-0.25	Crystalline	Considerable	10	<1
11	0.125-0.25	Granular	No	30	5
13	0.5-1.0	Crystalline	High	25	Nil
14	0.5-1.0	Crystalline	Very high	25	Nil

Table 2
Chemical composition of the Kora Gypsum deposit

Sample No.	IR %	R_2O_3 %	CaO %	MgO %	SO_3 %	H_2O %	LOI %
1	2.47	0.36	30.15	0.87	45.12	17.96	3.93
2	6.34	1.00	29.63	1.43	40.69	16.93	3.93
3	38.40	0.60	22.06	2.19	30.40	00.90	4.25
4	4.34	0.22	34.87	2.26	48.35	03.60	5.13
5	1.96	0.25	30.20	1.49	45.76	17.34	3.90
6	0.71	0.51	31.63	0.28	44.53	16.43	5.33
7	1.53	1.46	28.62	2.02	44.00	17.30	4.30
8	2.52	0.59	30.04	0.73	45.70	18.05	2.67
9	1.41	1.63	27.18	3.83	43.82	16.69	5.51
10	0.92	2.92	30.97	1.87	44.01	16.75	5.30
11	1.39	0.19	31.72	0.72	45.50	17.61	3.45
12	4.28	0.54	32.25	0.93	41.84	18.02	2.31
13	0.78	1.42	32.03	0.77	45.07	18.13	3.00
14	1.24	0.27	30.11	0.95	46.48	18.14	3.15
15	0.95	0.70	31.65	1.30	45.73	16.57	2.54
16	1.99	0.64	53.60	2.36	00.01	00.51	41.60
17	1.30	0.75	54.25	1.37	00.01	00.44	42.27

Table 3
Trace element assemblage of Kora Gypsum deposit

Sample No.	Na (ppm)	Al (ppm)	Fe (ppm)	Mn (ppm)	Ni (ppm)	Sr (ppm)	Zn (ppm)
1	90	530	950	20	15	1300	15
2	90	510	570	90	07	1820	15
3	1095	615	465	90	15	1540	15
4	120	700	900	80	17	1975	30
5	115	525	580	30	10	1600	15
6	120	175	355	35	15	665	15
7	115	250	490	35	20	1735	25
8	680	385	620	40	20	3190	20
9	110	265	660	50	00	515	20
10	935	190	385	60	20	745	25
11.	115	35	70	00	15	345	15
12	95	200	335	25	08	650	15
13	115	130	175	5	15	335	20
14	2360	75	125	10	20	450	20
15	270	115	200	00	10	425	20
16	660	345	380	20	20	1570	20
17	680	205	240	20	20	635	10

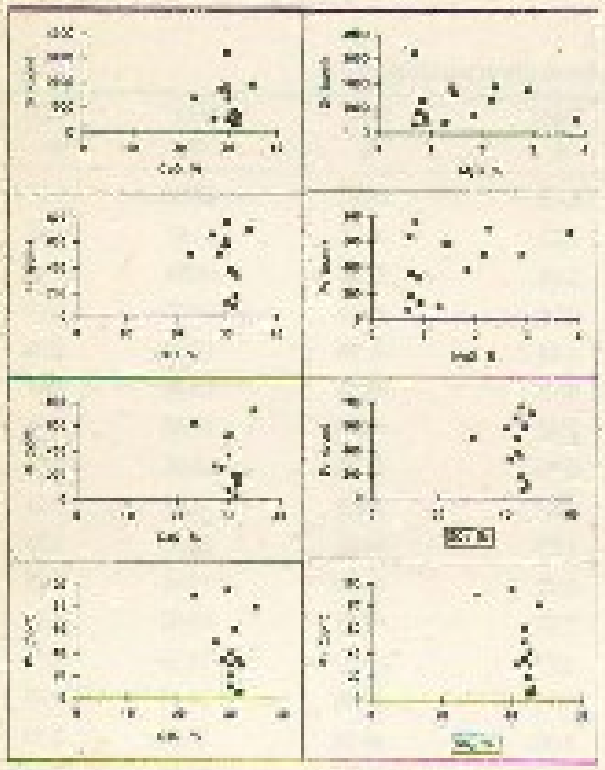

Fig 7. Degree of correspondence among major and trace elements. (Triangle represents Sakesar limestone)

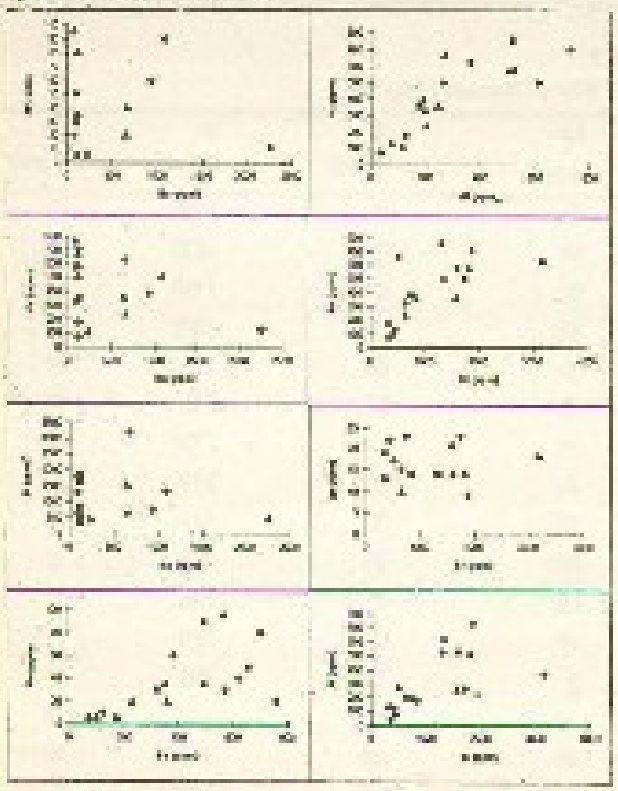

Fig 8. Degree of correspondence among major and trace elements.

ment is explained on the basis of gypsum structure. The most probable interstitial lattice position for trace ions in gypsum are among the water molecules. The space available is suitable for large ions (~ 1 Å). The ionic radius of gypsum is 1.13 Å and is close to fill the space between water molecule layers.

The plots of gypsum and limestone of the study area show nearly similar pattern of distribution of Sr vs Fe and Al. The relation is nearly positive linear (Fig 8). Sr shows very interesting relation with Zn. It shows gradual decrease from bottom to top samples. Probably the low enrichment of Zn in the study area samples is due to its low abundance in sea water (5 ppb) and its size (0.83 Å) is not fit in the interstices of gypsum water. The bottom samples have low consistency (<22 ppm) values possibly indicating loss of Zn during dewatering. The transformation of anhydrite to gypsum at top bank has further increased the concentration of Zn due to interaction with ground water.

The relation of Na vs Mn, Fe and Sr seems to be comparable. Sample 3, 8, 10 and 14 have relatively high content of Na (> 100 ppm). The rest of the samples show variable enrichment for close Na values. In spite of high abundance in sea water, (10,770 ppm) and favourable ionic size, Na has low PC in precipitate along with gypsum. This low PC further decreases with rising temperature (Ruskin 1980). Fe vs Al and Mn also displays corresponding patterns (Fig 8). The bottom samples show high Al probably due to the presence of higher amount of clay. The remaining samples exhibit gradual decline in the concentration of Al, Mn and Fe probably due to recrystallization.

Trace element concentration is valuable for facies analysis. Two samples (16 & 17) from Sakesar limestone from adjoining area have also been collected for this purpose. Average trace element abundance in limestone is 1,100 for Mn, 610 for Sr and 20 ppm for Ni and Zn. Both the limestone and gypsum show much higher Sr concentration. Aragonitic limestones contain Sr 7000-8000 ppm and during conversion to low magnesium calcite much of it is removed while gypsum may retain some of it. Mn and Fe are very low than the expected range. The low enrichment is probably due to faster rate of deposition in a deep basin.

It is important to note that the concentrations of Na, Sr, Al, Fe, Mn, Ni and Zn in limestone have similar distribution as in the gypsum-anhydrite facies. The plots of trace elements (Fig 8) show similar geochemical environment for gypsum and limestone. In the deep evaporitic basin possibly sulphate reducing bacteria convert gypsum into limestone (Friedman 1972) as a result the trace elements concentrations in both the facies remain similar.

Deposition model. Kendall (1984) has recognized the subaqueous evaporite deposits in deep water and shallow water facies. Ehrlich (1982) further categorized he deep water facies into Deep Basin-Deep Water (DBDW) and Deep Basin-Shallow Water (DBSW).

Thick deposition of evaporites is a distinctive characteristic of DBDW type of facies (Fig 4), the high rate of deposition (1Cm yr^{-1}). The Kara gypsum deposit is very thick it represent as a hill of pure gypsum deposit. According to Faure *et al* (1984), the study area at the time of deposition was present near equator, with high rate of deposition (Av. 15-20 mm yr^{-1}). Generally 1.5 cm thick salt is deposited by 100 mm evaporation of sea water (Schreiber 1986). One possible cause of high temperature in the basin was explained by Kendall (1983), according to him, sometimes the plastic limit in hypersaline water is reduced due to suspended organic residue, floating evaporite crystals and red anaerobic bacteria. Such turbid brines also trap radiant heat and the temperature may go up to 50°C. Another important evidence suitable for DBDW is the high subsidence rate. Basin subsidence in the major part of the Tethyan basin in tertiary was 0.1 mm yr^{-1} (Schreiber 1986). In the study area very thick deposition of younger siwaliks proves a high rate of sagging. The cross laminated and rippled sulphates are good indicator of shallow water deposits. Instead, the field observation favours DBDW facies because of thick crystalline laminae that is traceable over long distances. The presence of thin dark coloured clay, as described in petrography is also a clear evidence of DBDW facies. Latif and Iqbal (1986) concluded a barred basin in the area under study, which favours the flution of carbonate and evaporite facies (Fig 4). This type of facies is attributed to DBDW (Kendall 1983). Raup (1982) described another mechanism for the precipitation of gypsum. The experimentally induced precipitation of gypsum by mixing sea water brines of different compositions and salinities. Precipitation of gypsum would occur when brines mix at the interface between the dense basal layer and the less dense overlying layers. In the deep-sea situation only gypsum could precipitate in the central and deeper part of the buried basin.

Chalcophile elements (i.e. Zn, Ni, Cu) generally have no relation with evaporites. The samples under study showed Fe (70-700), Zn (10-23), Ni (7-20) and Cu (21-35) ppm. The enrichment of these elements in gypsum is also a function of DBDW facies, as described by Schmalz (1969) as follows. Due to conjunction high density water (1.1) cuts oxygen supply; as a result aerobic benthonic do not survive in the basin. This causes H_2S generation that reacts with base metal ions and causes sulphide mineral precipitation. Deep basin evaporites are marked by dark coloured organic-sulphide rich laminae/sediments.

The low Mg content and no K in the samples are also evidence of DBDW, whereas dolomite and dolomite-anhydrite are more in fore basin.

Conclusion

The early tertiary complex tectonics of the Salt Range uncovered separation of Kohat-Potwar and Sulaiman provinces as a result a close basin, suitable for the deposition of evaporites, was developed. During Lower Eocene, nine different formations were formed in the Salt and Surghar ranges with concentration of salt, shale, gypsum and limestone. In Dunkuld area the Sakesar limestone grades into gypsum deposits.

The petrographic study indicates fine granular anhydrite in the basal part and gradual conversion into coarse crystallized gypsum towards top beds. The gypsum crystals show replacement with anhydrite due to the interaction with ground water in the upper horizons. Gypsum grains show shearing and twisting as a result of anhydrite conversion to gypsum. Few samples also show remnants of anhydrite. Thin layers of dark clay are also observed which probably indicate Deep Basin Deep Water (DBDW) deposition conditions.

CaO shows good correlation with SO_3, but MgO does not indicate any genetic relationship. Low MgO content is good indicator of deep basin. Both Fe and absence of K is also a good evidence of DBDW.

Trace elements show variable concentration; depth, temperature, rate of sedimentation, thickness of evaporation sections and partition coefficients are mainly responsible for the distribution. However dehydration and recrystallization are the main phenomena.

Trace element ocean-Bays of the Sakesar limestone and SOD show close similarity.

Chalcophile elements (Fe, Zn, Cu & Ni) are sometime enriched as brecciated Sulphide rich sediments within evaporites. Their presence also indicate arid DBDW.

The plot of Ca/Mg vs Ca shows gradual deepening of the basin, indicating fast deposition rate and high subsidence in the basin.

The absence of mud cracks, cross laminations, rippled-structures and lack of dolomitization are also other evidences of DBDW type of model.

References

Adams J E 1971 Upper Permian Ochoa Series of Delaware Basin, West Texas and Southeastern New Mexico,

In *Origin of Evaporites*, AAPG Reprint series No. 2, pp 69-89.

Ahmad Z, Siddiqi R A 1993 *Gypsum and anhydrite*. In *Minerals and rocks for industry*. Geological Survey of Pakistan, Quetta, 2 pp 321-331.

Alam G S, Khan A J 1982 Gypsum and anhydrite deposits in Salt Range area Punjab, Pakistan. *Record Geological Survey of Pakistan* 59 p 45.

Burbank D W, Beck R A 1989 Early Pliocene uplift of the Salt Range; Temporal constraints on thrust wedge development southwest Himalaya, Pakistan. In: *Tectonics of the western Himalayas* eds Malinconico L L, Lillie R J, The Geological Society of America, Special paper 232 pp 113-123.

Butler G P 1969 Modern evaporite deposition and geochemistry of coexisting brines, the sabkha, Trucial Coast, Arabian Gulf. *Journal of Sedimentary Petrology* 39 70-89.

Einsele G 1992 *Sedimentary Basin* Evolution, Facies and Sedimentary Budget. Springer-Verlag, London pp 628.

Farah A, Lawrence R D, Lyons K A 1984 An overview of the Tectonics of Pakistan ed. In *Marine Geology and Oceanography of Arabian Sea and Coastal Pakistan*. Haq B U, Milliman J Deas Van Nostrand Reinhold Company/ Scientific and Academic Editions pp 161-176.

Friedman G M 1972 Significance of Red Sea in problem of evaporites and basinal limestones. *AAPG Bulletin* 56 1072-1086.

Gee E R 1960 *Pakistan Geological Salt Range Series, Sheet 1, Scale 1:50,000*. Directorate of Overseas Survey, U K.

Gee E R 1989 Overview of the geology and structure of the Salt Range with observations on related areas of northern Pakistan. In *Tectonics of the western Himalayas* eds Malinconico L L, Lillie R J. The Geological Society of America, Special paper 232 pp 95-112.

Goldsmith L H 1989 Concentration of Potash salts in saline basin. *AAPG Bulletin* 83 709-727.

Jowett E C, Cathles I M, Davis B W 1993 Predicting depth of gypsum dehydration in evaporite sedimentary basins. *AAPG Bulletin* 77 402-413.

Kazmi A H, Jan M Q 1997 *Geology and Resources of Pakistan*. Graphic Publishers, Karachi, p 354.

Kendall A C 1985 Salina group Evaporites. Walker R G ed. Facies Models. Geoscience Canada Reprint Series 1, Geological Association of Canada, p 139-174.

Kushair I 1988 The coprecipitation of strontium, magnesium, sodium, potassium and chloride ions with gypsum. *Geochemica et Cosmochimica Acta* 44 1471-1482.

Latif M A, Iqbal T 1986 Lithologic studies and a tentative correlation of a barrier, separating the Sulaiman and Kohat-Potwar Provinces of Indus Basin, Pakistan during Lower Eocene. *Karachi Journal of Geology* 4 123-133.

McDougall J W, Khan S H 1990 Strike-slip faulting in a foreland foldthrust belt the Kalabagh fault and western Salt Range Pakistan. *Tectonics* 9 1061-1075.

Raup O B 1982 Gypsum precipitation by mixing seawater brines. *AAPG Bulletin* 66 161-167.

Schmalz R F 1969 Deep water evaporite deposition: A Genetic Model. *AAPG* 53 798-823.

Stoss L L 1969 Evaporite deposition from layered solutions. *AAPG* 53 736-749.

Yeats S R, Khan S H, Akhtar M 1984 Late quaternary deformation of the salt range of Pakistan. *Geological Society of America Bulletin*. 95 958-966.